Modelling of the rheological behaviour of slurries used for cold transportation

Myriam Darbouret, Michel Cournil, Jean-Michel Herri

XI° Congrès de la Société Française de Génie des Procédés. Des réponses industrielles pour une société en mutation. Saint Etienne, 9 au 11 octobre 2007, N°96, 2-910239-70-5

Modelling of the rheological behaviour of slurries used for cold transportation

DARBOURET Myriam[b], COURNIL Michel[a], HERRI Jean-Michel[a*]

[a] *ENSM-SE, Centre SPIN, Département GENERIC, LPMG (UMR CNRS 5148) 158, Cours Fauriel, 42023 Saint-Etienne Cedex 02*

[b] *IFP-Echangeur Solaize 69360 SOLAIZE*

Abstract

Suspensions of solid crystals are used for cold transportation purposes with the aim of reducing the use of classical refrigerants. From a general point of view, the understanding and the mastering of the rheological properties of the crystal suspensions is essential for controlling the operating conditions. Water ice and Tetra-ButylAmmonium Bromide (TBAB) hydrate aqueous give rise to non-Newtonian flows. In particular Bingham-like behaviours are frequently observed. Two reasons at least can explain deviation from Newtonian characteristics: crystal agglomeration and particle.

Keywords:

rheology ; slurries ; hydrates ; cold transportation ; crystallization

1. Introduction

Secondary two-phase fluids are suspensions of solid crystals. Thanks to their high melting latent heat, they present a great interest for cold transportation. Moreover, they are a mean of reducing the amount of classical refrigerants such as CFC, HFC, which may have a harmful effect on the environment. In the refrigeration field, ice slurries are frequently used, because in presence of additives negative temperatures can be easily reached. For applications to air-conditioning, however, the required temperature should range between +6°C and +12°C. In these conditions, use of a solid compound with phase transformation temperature in the same domain is necessary. Hydrate crystals which are structurally similar to water ice are good candidates for this application, because they are formed at positive temperatures. In both cases, the main problem is to prepare slurries as concentrated as possible in ice or hydrate crystals, however with transport properties which remain compatible with their use in the refrigeration or air-conditioning loops.

In this work, we present the experimental results obtained for slurries of ice water in a commercial refrigerant fluid (HYCOOL-25), on the one hand, of TBAB (Tetra-ButylAmmonium Bromide) hydrate crystals, on the other hand. We particularly focus our interest on the rheological properties of these suspensions according their yield in solid. Non-Newtonian behaviours are systematically observed. This is a frequent situation in the case of concentrated slurries. Literature provides us with two main tracks of interpretation that are explored in this paper:

- In this work, the investigated two-phase media are in conditions of saturation or supersaturation as regards the solid-liquid equilibrium; this is a favourable situation for agglomeration of crystals. Influence of particle-particle interactions on the rheology of suspensions has been extensively studied, particularly in the case of metal oxide aqueous suspensions (Firth, 1976; Firth and Hunter, 1976a; Firth and Hunter, 1976b; Firth, 1980).

[*] Corresponding Author: herri@emse.fr

These authors have developed different theoretical approaches, generally known under the name of "elastic floc" models.

- For one of the investigated suspensions (water ice in aqueous solution), there is a significant difference between the density of the solid phase and the liquid phase. Consequently, floating of crystals may be expected and result in stratified flows. Two-and three-layer models for solid-liquid flows in horizontal and pipes have been proposed by (Doron and Barnea, 1987; Doron and Barnea, 1993; Doron and Barnea, 1995; Doron and Barnea, 1996).

Present paper is structured as follows: first, material and methods are described, then, main results of the rheological study of water ice and TBAB suspensions are presented; in last section, these results are interpreted in the framework of the existing models. Numerical simulations are necessary in the case of the Doron and Barnea approach. Thanks to these different models, we expect to facilitate the choice of operating conditions and dimensions of the cold transportation installations.

2. Material and methods

In this section we present first the two solid-liquid systems investigated in this research.
Then we describe the set-up of production and rheological characterization of the slurries and give indication on the way of exploiting the experimental results. More detailed description can be found in (Darbouret, 2005).

2.1 Slurries

HYCOOLTM is a cooling fluid marketed by HydroCool, the cooling agent division of the Norwegian company NORSK HYDRO. It is currently used in the secondary loops of refrigeration as a monophasic refrigerant. Its composition is adjusted according to the application considered because its temperature of crystallization must always be lower than the minimal temperature of use. Consequently, HydroCool markets various solutions according to the temperature of desired crystallization. We worked with HYCOOL-25, whose temperature of crystallization is - 25°C. It is an aqueous solution of potassium formiate (33% in mass) and anti-corrosion additives. Some of its physical properties are reported in Table 1.

Table 1. Physical properties of HYCOOL-25 .

Temperature [°C]	Density [kg.m^{-3}]	Dynamic viscosity [mPa.s]
20	1213	1.85
10	1217	2.29
0	1222	2.93
-10	1226	3.88
-20	1231	5.32
-25	1233	6.34

It appears clearly that this fluid is notably denser than pure liquid water and that consequently the crystals of water ice (917 kg.m-3 at 0°C) will have a more pronounced trend to float. In addition at the lowest temperatures, HYCOOL-25 is much more viscous than water (1 mPa.s at 20°C).

Solid TBAB consist of white crystals. It is very water soluble (solubility mass fraction 0.60 in mass at 20°C). TBAB hydrates crystallize in clathrate-like structures. Two types of hydrates, A and B, differing by their number of hydration, respectively 26 and 38, are observed. We could determine experimentally the solid-liquid equilibrium temperatures according to the mass fraction XTBAB in dissolved TBAB (Table 2). Their mass enthalpy of dissociation, respectively, 193 kJ.kg-1 and 199 kJ.kg-1 -to compare with the enthalpy fusion ice (333 kJ.kg-1) make of them compounds energetically interesting for air-conditioning.

Table 2a. Equilibrium conditions in the Water - Tetra-ButylAmmonium Bromide (TBAB hydrate) system

X_{TBAB}		0.50	0.40	0.30	0.25	0.20	0.15	0.10	0.05
T_{fusion}	Hydrate A	12.1	12.4	12.1	11.1	9.6	6.5	2.9	-0.4
[°C]	Hydrate B					9.6	8.8	7.5	1.7

Table 2b. Physical properties of TBAB solutions

X_{TBAB}	Temperature [°C]	Density [kg.m^{-3}]	Dynamical viscosity[mPa.s]
0.15	22	1011	2.8
	9	1017	3.6
0.20	16	1020	4.0
	9	1022	4.0
0.35	18	1033	5.5
	13	1037	5.1
0.50	24	1038	9.0

2.2 Experimental set-up

A schematic representation of the experimental set-up is shown in Figure 1. The ice or hydrate slurries are generated in a 3 L stainless steel double-jacketed reactor. Low temperature is ensured by means of a methanol cryostat. The new solid particles crystallize on the internal cold surface and are released to the bulk by continuous brushing. They are then put in circulation in a loop by means of a gear pump.

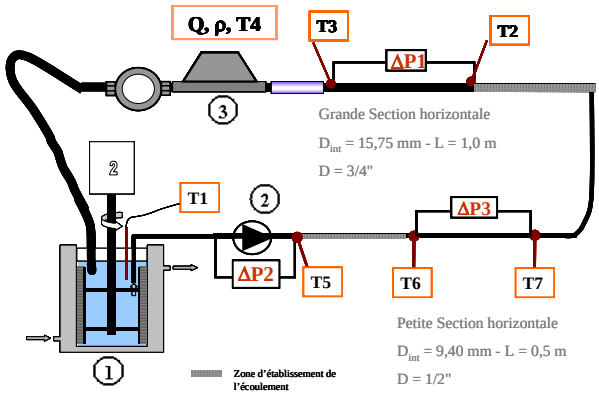

Figure 1. Schematic representation of the experimental set-up

The loop itself includes two successive cylindrical pipes of respective outer and inner diameters and length: ¾ ‘’, 16 mm and 1m (T3-T2 portion), and ½’’, 9.4 mm and 0.5 m (T6-T7 portion). This circulation line is provided with differential pressure sensors and Pt 100 temperature sensors (± 0,1°C) (T1, T2, T3, T6, T7). Flow-rate is measured using a Coriolis flow meter which is particularly adapted to measurements on two-phase flows. The whole of the installation is insulated with foam, in order to limit the thermal transfers with the exterior medium. In each experiment, the main action factors that the operator can adjust are the slurry concentration in solid via the cryostat temperature and the slurry flow rate via the gear pump rotation rate.

2.3 Determination of the slurry content in solid particles.

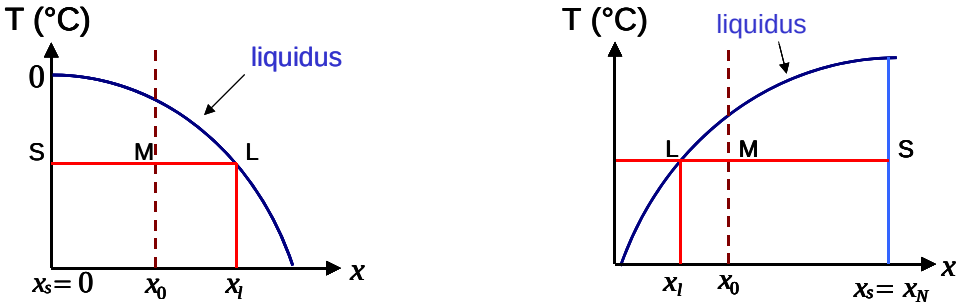

a- *b-*

Figure 2. Principle of method of moments a- ice/HYCOOL-25, b- TBAB hydrates/ TBAB solution

3. Rheological behaviour of water ice and TBAB hydrate slurries

The rough experimental results are available as curves of evolution of linear pressure drop $\frac{\partial P}{\partial z}$ versus mean velocity $\bar{U}$ of the fluid for various values of the concentration in particles. It will be more interesting to work on transformed curves of the preceding ones. For this purpose, some recalls of rheology are essential (Midoux, 1993).

3.1 Elements of rheology

The rheological models are expressed in general in the form of a relation between speed shearing rate $\dot{\gamma}$ and shear stress τ. For example, for a Newtonian viscous fluid, $\tau = \mu\dot{\gamma}$. Power laws like the Ostwald van de Waele model are met too:

$$\tau = k\dot{\gamma}^n \tag{1}$$

as well as the model of Bingham which is representative of the rheological behaviour of many slurries (Figure 3):

$$\begin{cases} \tau \le \tau_0 & \dot{\gamma} = 0 \\ \tau > \tau_0 & \tau = \tau_0 + \mu_0\dot{\gamma} \end{cases} \tag{2}$$

where μ_0 is called *plastic viscosity* of the fluid and τ_0 is the *shear stress threshold* beyond which the fluid can be put in motion.

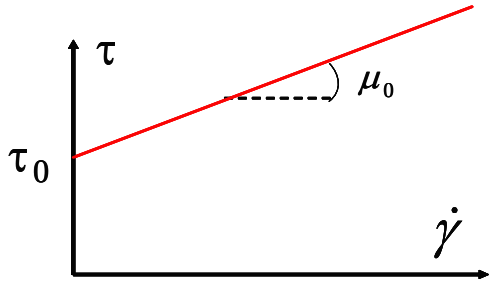

Figure 3. Bingham fluid rheology

For a flow in a horizontal cylindrical line of diameter D and length L, the shear stress in the pipe, $\tau(r)$, at radius r, is expressed versus the shear stress on the wall τ_w.

$$\tau(r) = \frac{\Delta P}{2L} r = \tau_w \frac{2r}{D} \text{ and } \tau_w = \frac{D\Delta P}{4L} \tag{3}$$

In the particular case of a Bingham fluid, the plastic viscosity and the shear stress threshold can be easily deduced starting from the plot representing the shear stress on the wall $\tau_w = \frac{D}{4}\frac{\Delta P}{L}$ versus the shearing rate $\Gamma_w = \frac{8\bar{U}}{D}$. One obtains in this case a straight line of slope μ_0 and intercept $\frac{4}{3}\tau_0$.

In the particular case of Ostwald-van de Waele fluids, $\ln(\tau_w)$ is a linear function of $\ln(\frac{8\bar{U}}{D})$ and

$$n = \frac{d\ln(\tau_w)}{d\ln(\frac{8\bar{U}}{D})} \qquad (4)$$

3.2 Water ice slurries in HYCOOL-25

In Figure 4 are reported typical flow diagrams obtained for ice slurries at different concentrations in solid (Φ, volume fraction in ice). Straight lines are obtained. Thus, it appears that the Ostwald-van de Waele model is quite representative of the behaviour observed.

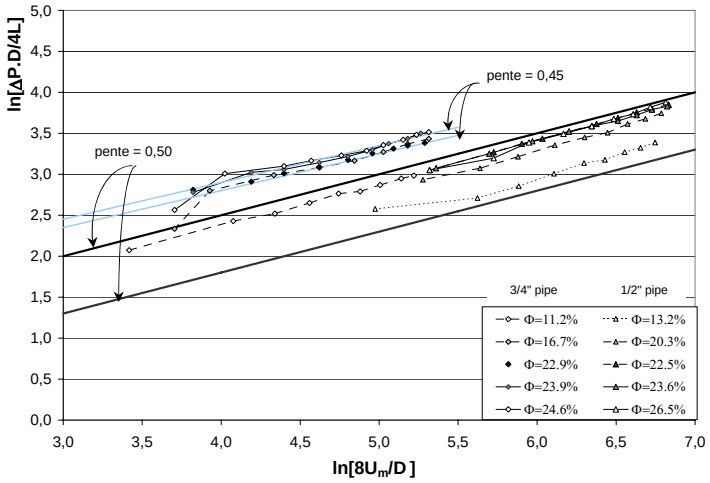

Figure 4. Graphical validation of Ostwald-van de Waele model for ice slurries

In Table 3, the different values obtained for *n* are reported. They are independent of the volume fraction in solid, however they seem to depend on the tube diameter (for reasons which are not clear so far).

Table 3. Values of rheological parameter n of different ice slurries

½" pipe					
Φ	13.2%	20.3%	22.5%	23.6%	26.5%
n (±0.01)	0.50	0.50	0.50	0.50	0.50
¾ " pipe					
Φ	11.2%	16.7%	22.9%	23.9%	24.6%
n (±0.01)	0.50	0.45	0.45	0.45	0.45

These results are similar to those obtained by (Ben Lakhdar, 1998) for ice suspensions in ethanol-water solutions at concentrations above 10%.

3.3 TBAB hydrate slurries

As explained before, in order to confirm the expected Bingham behaviour, we have plotted $\tau_w(\Gamma_w)$ curves obtained for different concentration in TBAB hydrates and for pipe diameter ¾ '' (Figure 5).

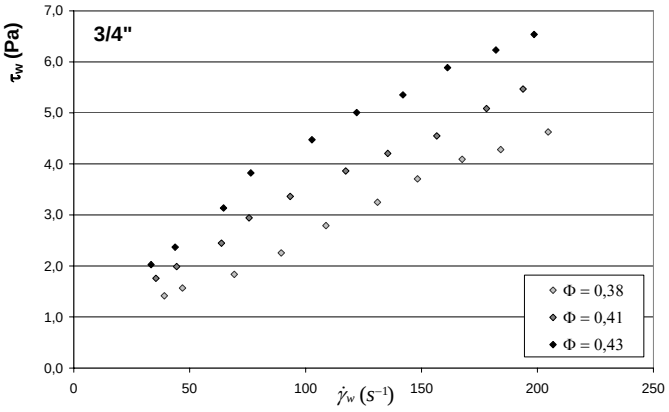

Figure 5. Graphical validation of Bingham model for TBAB hydrate slurries

Linear variation, however with non zero intercept, confirms the Bingham law validity. As aforesaid, both plastic viscosity μ_0 and threshold shear stress τ_0 can be derived from such diagrams. Their respective variation versus Φ are represented in Figures 6 and 7. Dynamical viscosity seems to diverge when Φ tends to a limit value. Threshold shear stress is very low for hydrate yield lower than 20%, and then rapidly increases.

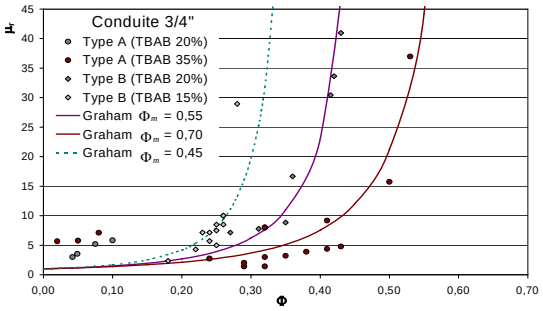

Figure 6. Relative viscosity of TBAB-hydrate slurries versus volume fraction in solid

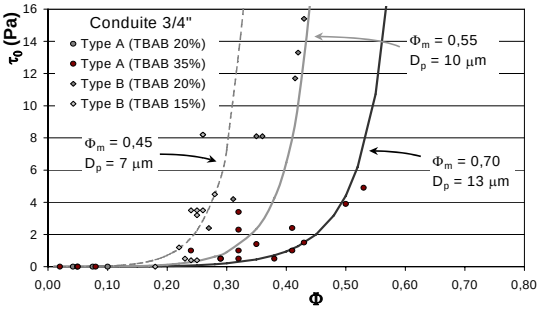

Figure 7. Threshold shear stress versus volume fraction in TBAB-hydrate

4. Interpretation

Different aspects of the previous rheological behaviours are examined in the framework of models.

4.1 Viscosity of the TBAB-hydrate slurries

The model of Graham, (Steele and Bird, 1984) is applied successfully (solid lines in Figure 6). Coinciding with the model of Einstein for low contents in solid, it takes into account the volume fraction of maximum packing Φ_m which represents the limit for which all the particles come into contact, the suspension then tending to behave like a solid. For this limit value, the suspension viscosity diverges. Model predictions are as follows:

$$\mu_0 = \mu_l \left(1 - V_0 \Phi\right)^{-2,5} \text{ with } V_0 = 1 + \left(1/\Phi_m - 1\right)\left[1 - \left(1 - \Phi/\Phi_m\right)^2\right]^{1/2} \quad (5)$$

For type A hydrate, maximum packing ranges between 0.70 and 0.74, *i.e.* values corresponding to compact packing of spheres. For type B hydrate, Φ_m =0.50, which indicates a looser packing.

4.2 Threshold shear stress for TBAB-hydrate slurries

The approach recommended by (Firth and Hunter, 1976 a and b, 1980) is used here. When the suspension is little concentrated, each particle evolves/moves as if it were alone in the carrying medium. When the content of particles increases, interactions between particles become more frequent and a threshold stress can arise, which increases with the frequency of the interactions and their intensity. If the van der Waals attraction forces between crystals are sufficient to overcome the constraints exerted by shearing, aggregates can be formed. Van der Waals force F_A is given by:

$$F_A = \frac{A}{24 D_p \left[\left(\frac{\Phi_m}{\Phi}\right)^{1/3} - 1\right]^2} \quad (6)$$

where A is the Hamaker constant calculated in (Darbouret, 2005) and D_p the crystal equivalent diameter.

Moreover, the number of shocks between particles per unit of time and volume is estimated by:

$$n_c = \frac{24 \Phi^2 \dot{\gamma}}{\pi^2 D_p^{\,3}} \quad (7)$$

The total energy dissipated by theVan der Waals interaction between the suspended particles per unit of time and volume is expressed then in the form:

$$E_A = n_C F_A = \frac{A \Phi^2 \dot{\gamma}}{\pi^2 D_p^{\,4}} \left(\left(\frac{\Phi_m}{\Phi}\right)^{1/3} - 1\right)^{-2} = \tau_0 \dot{\gamma} \quad \text{hence} \quad \tau_0 = \frac{A \Phi^2}{\pi^2 D_p^{\,4}} \left(\left(\frac{\Phi_m}{\Phi}\right)^{1/3} - 1\right)^{-2} \quad (8)$$

The diameter of the particles is experimentally difficult to reach. It is actually estimated by fitting between the preceding equation and the experimental results such as those represented in Figure 7. In this Figure the good adequacy of the model can be judged.

4.3 Influence of crystal creaming on the rheology of ice slurries

As aforesaid, relative density difference between ice crystal and liquid phase (HYCOOL) in ice slurries is relatively high (25%). It causes a notable creaming phenomenon which results in the stratification of the flow. In concentrated suspensions, a layer of solid particles in the upper part of the pipe brings about significant friction, thus deviation from Newtonian behaviour.

We present here the principles of the corresponding model which is widely inspired by the (Doron and Barnea, 1987; Doron and Barnea, 1993; Doron and Barnea, 1995; Doron and Barnea, 1996) works on stratified slurry flows. Figure 8 represents the formation of the particle bed.

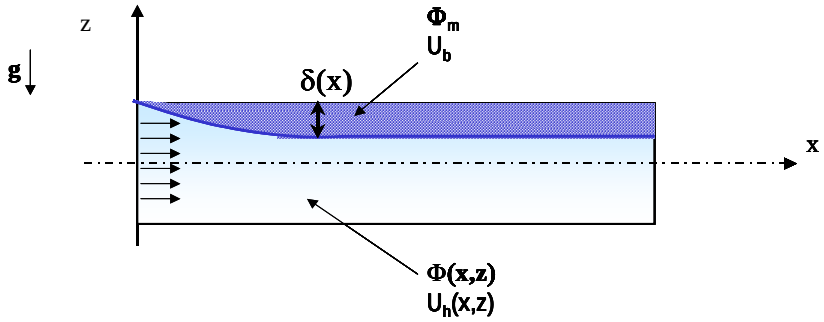

Figure 8. Ice crystal bed formation on the pipe upper part

In some cases, (Doron and Barnea, 1987; Doron and Barnea, 1993; Doron and Barnea, 1995; Doron and Barnea,, 1996) consider that the upper part of the particle bed may be fixed whereas the lower part is mobile. Visual observations never show the presence of a fixed bed, thus, the schematic representation of the solid concentration and velocity profiles in the pipe (Figures 9a and 9b).

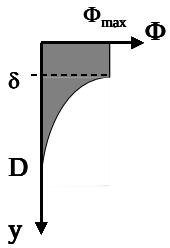

Figure 9 a. Solid particle concentration profile in pipe

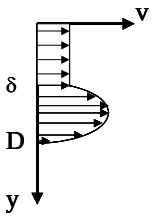

Figure 9 b. Velocity profile in pipe

In stationary conditions, the model consists of the following equations (details can be found in (Darbouret, 2005):

Momentum balance

$$\begin{cases} \dfrac{\partial P}{\partial x} \approx \dfrac{\partial}{\partial z}\left(\mu_0(\Phi) \dfrac{\partial U_x}{\partial z} \right) \\ \dfrac{\partial P}{\partial z} \approx -\rho^m g \end{cases} \qquad (9)$$

U_x, is the axial velocity, ρ^m, the mixture density, g, the gravity.

Mass balance

$$A\bar{\Phi}\bar{U} = A_b\Phi_m U_b + \int_{A_h} \Phi(x,z)U(x,z)dz \qquad (10)$$

A is the total flow section area, $\bar{\Phi}$, the input mean concentration in solid, $\bar{U}$, the input mean velocity, U_b, the velocity of the mobile bed, A_b, its section area, and Φ_m, the solid concentration in the bed.

$$\frac{\partial}{\partial x}\left(U(x)\Phi(x,z)\right) = \frac{\partial}{\partial z}\left(D(x,z)\frac{\partial\Phi(x,z)}{\partial z}\right) - \frac{\partial}{\partial z}\left(w(x,z)\Phi(x,z)\right) \qquad (11)$$

This continuity equation contains D, the (Leighton and Acrivos, 1986) diffusion coefficient and w, the creaming velocity of the crystals (Richardson and Zaki, 1954):

$$D \approx \frac{\dot{\gamma}D_p^{\,2}}{12}\Phi^2\left(1+\frac{1}{2}\exp(8{,}8\Phi)\right) \qquad w = \frac{D_p^{\,2}(\rho_s-\rho_l)\,g}{18\mu_l}\left(1-\frac{\Phi}{\Phi_m}\right)^n$$

Boundary conditions: they describe the mobile bed dynamics submitted both to the shearing effect of the fluid and the friction on the wall. For lack of space, they are not given here (Darbouret, 2005).

Numerical simulations: Finite differences algorithms are applied to this free-boundary problem. They are detailed in (Darbouret, 2005). Figure 10 shows an example of calculated velocity and concentration profiles. In Figure 11 are reported different rheological diagrams.

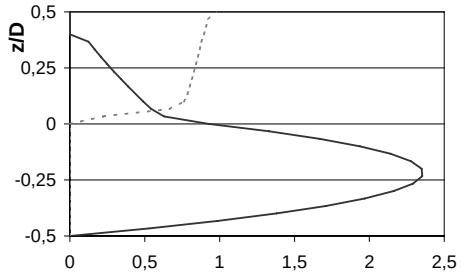

Figure 10. Calculated concentration and velocity profiles in case of ice crystal mobile bed

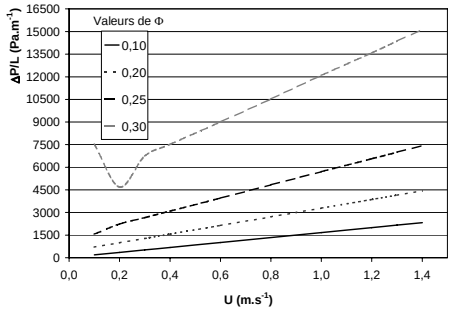

Figure 11. Calculated rheological diagram in case of ice crystal mobile bed

References

Ben Lakhdar, M. A. 1998. Comportement hydrodynamique d'un fluide frigoporteur diphasique : le coulis de glace. Etude théorique et expérimentale. Ph. D. Thesis, Thermique et Energétique, Ecole Doctorale de Lyon (France)

Darbouret, M., 2005. Etude morphologique d'une suspension d'hydrates en tant que fluide porteur diphasique. Résultats expérimentaux et modélisation. Ph. D. Thesis, Ecole Nationale Supérieure des Mines de Saint-Etienne (France)

Doron, P., D. Barnea, 1987. Slurry flow in horizontal pipes-Experimental and modelling. International Journal of Multiphase Flow 13, 535.

Doron, P., D. Barnea, 1993. A three-layer model for solid-liquid flow in horizontal pipes. International Journal of Multiphase Flow 19, 1029.

Doron, P., D. Barnea, 1995. Pressure drop and limit deposit velocity for solid-liquid flow in pipes. Chemical Engineering Science 50, 1595.

Doron, P., D. Barnea, 1996. Flow pattern maps for solid-liquid flow in pipes. International Journal of Multiphase Flow 22, 273.

Firth, B.A., 1976. Flow properties of coagulated colloidal suspensions. I. Energy dissipation in the flow units. Journal of Colloid and Interface Science 57, 248.

Firth, B.A., R.J. Hunter, 1976a. Flow properties of coagulated colloidal suspensions II. Experimental properties of the flow curve parameters. Journal of Colloid and Interface Science 57, 257.

Firth, B.A., R.J. Hunter, 1976b. Flow properties of coagulated colloidal suspensions. III-The elastic floc model.. Journal of Colloid and Interface Science 57, 266.

Firth, B.A., R.J. Hunter, 1980. Flow properties of coagulated colloidal suspensions V. Dynamics of floc growth under shear. Journal of Colloid and Interface Science 76, 107.

Graham, A.L., R.D. Steele, R.B. Bird, 1984. Particle clusters in concentrated suspensions. 3. Prediction of suspension viscosity. Ind. Eng. Chem. Fundam. 23, 420.

Leighton, D., A. Acrivos, 1986. Viscous resuspension. Chemical Engineering Science 41, 1377.

Midoux, N., 1993. Mécanique et rhéologie des fluides en génie chimique. Lavoisier, Paris.

Richardson, J.F., W.N. Zaki, 1954. Sedimentation and Fluidisation: Part 1. Trans. Inst. Chem. Eng. 32, 35-53